Purlin-Cladding interaction in standing seam roofs

Mansour Kachichian / *László* Dunai

Abstract

The research activity presented in this paper focuses on the effect of sliding clips and intermediate elements (bridge system) on the secondary load-bearing beams (Z-purlins) in standing seam roofs. The main aim is to determine the lateral stiffness of the system to be used in the stability checking of Z-purlins. The representing element of the roof system is built in the Structural Laboratory of the Budapest University of Technology and Economics (BME), Department of Structural Engineering. The specimens are built with Z-purlin and MR24 aluminium panels connected to each-other with the help of the concealed sliding clips using folding technique, without holes on the outer surface. The interaction is experimentally studied between the purlin and the cladding system assembly, and the lateral stiffness of the system is interpreted and determined from the test results. The effects of the gravity load on the panels and the different components on the lateral stiffness of the roof system are determined and evaluated.

Mansour Kachichian

BME Department of Structural Engineering, H-1111 Budapest Műegyetem rkp. 3, Hungary

e-mail: mkachichian@epito.bme.hu

László Dunai

BME Department of Structural Engineering, H-1111 Budapest Műegyetem rkp. 3, Hungary

1 Introduction

1.1 Previous investigations

The cladding system used in the current analysed structural layout of the standing seam roofs are built by the application of panels connected to sliding elements which are fixed to the Z-purlins with or without intermediate elements (bridge system). This cladding has one of the most exciting breakthroughs in the roofing technology in the last decades, because of the benefit gained from this system, like puncture resistant against weathering conditions (weather tightness, durability), light weight, easy to install and to maintain, reliable, energy efficient, corrosion resistant, recyclable and the erection is cost-effective.

The previous investigations available in literature in this topic are focusing (i) on the individual elements of the standing seam roof system, and (ii) on the whole system, by the testing of full scale specimens. In the followings an overview is given on the previous studies.

In the experimental research of Serrette and Peköz in 1997 a prediction model was developed to determine the maximum load bearing capacity of the panels, clips and Z-purlin systems under vertical load [1]. In the experiments two different panel types were investigated and the load was applied by vacuum to simulate the vertical load until reaching the ultimate load. The ultimate loads of the full scale specimens were determined in the tests and the results were compared to the analytical values.

In frame of a research program full scale standing seam roof specimens were tested in wind tunnel by Surry et al, in 2007 [2]. On the bases of these tests a numerical model was developed and designed with targeted failure at clips by Farquhar et al. [3]. The goal of the study was to characterize the relationship between uniform uplift pressure used in standard test procedures and the dynamic pressures that occur during real wind loading that cause failure.

Three dimensional static and dynamic analyses were carried out by Ali and Senseny in 2003, to analyze the effect of the geometry and boundary conditions for the roof panels, seams, clips, fasteners and purlins. Preliminary results of this research program are available in [4]. Numerical investigations are executed by El Damatty et al, in 2003 [5], to investigate the struc-
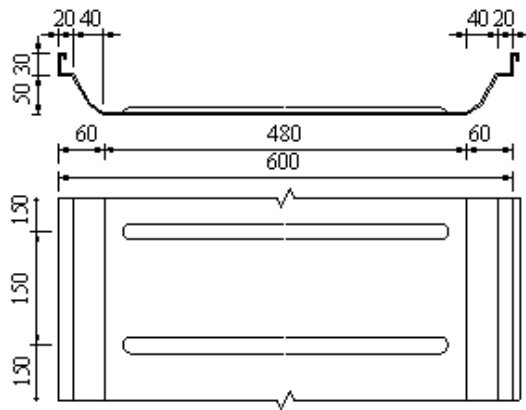
Fig. 1. Geometry of the MR24 panel.

tural behaviour of the clips and seams under uplifting wind load. A finite element model was developed where the purlins were modelled using beam elements and the clips and seams by equivalent springs. This numerical model was verified based on the full scale model tests mentioned before.

In the above detailed investigations the standing seam roofs were analyzed using only clips, without intermediate elements (bridge system). In the current research program specimens with bridge systems are also tested, considering the sliding action which was not taken into account in the previous investigations.

1.2 Components of specimens

Two types of Z-purlins are used during the tests, with a height of 200 and 250 mm (Z-200 and Z-250). The cladding element is an aluminium panel with 600 mm width (MR24 panel), as shown in Fig. 1. These panels are fixed to the purlins through sliding clips without holes on the surface.

The sliding clips have two components: (i) one is fixed to the purlins, and (ii) the other can move in longitudinal direction, as shown in Fig. 2. These sliding clips are folded together to get the roof system, as shown in Fig. 3. The non-moving end of the sliding clip is connected either to the purlin directly or to the intermediate bridge system.
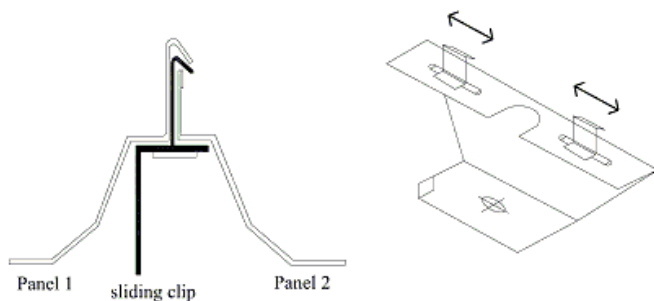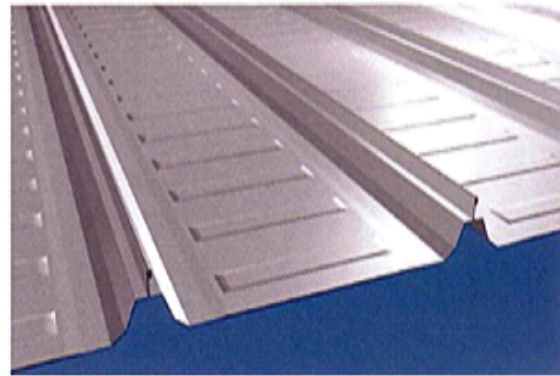

Fig. 2. Sliding clips in the purlin/MR24 panel connection.

The bridge system has two components: (i) bridge clip (or bridge support), and (ii) bridge bar (or bridge beam), as shown in Fig. 3. The bridge bar is fixed to the sliding clips, and the bridge clips are fitted into the bridge bar then the foot of the bridge clip is fixed to the Z-purlins. If bridge system is not used the

sliding clip is connected to the purlin directly. Standing alone sliding clips and sliding clips with bridge system have the main function to transfer the loads from the panels to the purlins as concentrated loads.
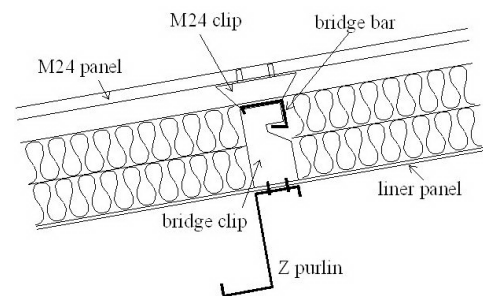

Fig. 3. Sliding clip with bridge systems in purlin/MR24 panel connection.

1.3 Aims and scopes

The upper flange of the purlin has conditional lateral support due to the sliding phenomenon which has significant effect on the stability behaviour of it. The resulted uncertainties in the lateral stiffness should be considered in the stability checking of the purlins. The characteristics of the interacting behaviour between the purlin and the cladding are not clarified in the literature.

In the current experimental research the standing alone sliding clips and sliding clips with bridge are studied in the Z-purlin/MR24 cladding system. The clips and bridges give a conditional lateral support to the upper flange of the purlin which affects the distortional and lateral torsional buckling modes. The aim of the current study is to clarify the complex structural behaviour and the effects of the system components on it. Two test series with different structural layouts – with bridges and without bridges – are investigated, loaded by adjustable roof gravity loads (vertical loads) in addition to the lateral loads.

The total of 182 test specimens is examined. From the obtained experimental results the structural behaviour of the specimens are determined and characterised. The lateral displacements are measured and based on the experimental results the lateral stiffness is defined and calculated. The lateral stiffness

is interpreted on the basis of the EN 1993-1-3 [6] proposal, and extended according to the novel structural arrangement. The stiffness results obtained from the proposed models are applied in the global stability analysis and design of the Z-purlins by the industrial partner.

2 Research program

2.1 Test specimens and test arrangement

The specimens are built from the combinations of two types of purlins (Z-200 and Z-250), one type of panel (M24), sliding clips, glass-fibre blanket and bridge system. Two specimen groups are constructed: (i) one is built without bridge system, and (ii) the second series is built with bridges, as shown in Fig. 4.

In each specimen series two purlin heights are used: 200 and 250 mm. Four load conditions are studied containing lateral and vertical load combinations, as presented in Fig. 4. During the tests for each specimen the magnitude of the vertical load is kept constant. Five different vertical load magnitudes are applied and the lateral load is enlarged during the tests. The used vertical load intensities: 0, 165, 427, 577, and 727 N/clip.

The test arrangement is planned according to EN 1993-1-3 [6], considering the specialities of the novel structural detail. This setup is used for the lateral stiffness testing of the restrained and the unrestrained (free) flanges of the purlins, where the upper flange is the free and the lower one is connected to the panel system. Panels are fixed to wooden spacings which are fixed to the main supporting system. Self-drilling screws are used to fix the panels to the wooden spacing. The layout of specimen is shown in Fig. 5. The wooden spacing has the function to prevent the local displacements at the edges of panels through the loading procedure.

2.2 Loading and measuring system

The test specimens are laterally loaded at two levels and vertically at the top of the upper flange. The applied loads, the load combinations and the positions of the measured deformations are shown in Figs. 5 and 6. The executed tests can be ordered into four different loading series based on the applied loading situations and the support conditions. These are expressed in the function of F_T, U_T; F_B, U_B and F_V where U_T and U_B are the average values of the three measured displacements (U_{T1}, U_{T2}, U_{T3}) and (U_{B1}, U_{B2}, U_{B3}), and they are summarised as follows:

- Lateral load F_T is applied at the top of the upper flange, and the corresponding average lateral displacement U_T is measured at the upper flange of the Z-purlin (loading type 1).

- Lateral load F_B is applied at the level of lower flange, and the corresponding average lateral displacement U_B is measured at the height of 1/6 of the web height (loading type 2).

- Lateral load F_B is applied at the level of lower flange, vertical load at the upper flange F_V, and the corresponding average lateral displacement U_B is measured at the level of the 1/6 of the web height (loading type 3).

- Lateral load F_B is applied at the level of lower flange, vertical load F_V at the upper flange, and the corresponding average lateral displacement U_B is measured at the level of the 1/6 of the web height. In the series the specimens are supported at the upper flange as well (loading type 4).

Beside the above lateral displacements the vertical deflections of specimens are measured at the lower surface of the panel at mid-span.

2.3 Testing procedure

The instrumentation has been implemented in order to determine and define the lateral stiffness of the standing seam roofs with sliding clips and to check the effect of sliding clips, bridge systems, vertical loads and restrain of the upper flange, on the bases of the measured lateral load and displacement (F_i–U_i) relationships. In the tests two types of loading procedure are used, as follows:

In case of specimens loaded with combination of lateral and vertical loads, the vertical load is placed first with the whole magnitude and it is kept constant during the tests. The lateral load is applied after it and continuously increased. The maximum load is considered to be when h/10 displacement is reached in case of upper flange loaded (F_T). When the lower flange is loaded (F_B) the maximum load is considered to be when the maximum sliding capacity is reached. The applied load and the corresponding displacements are measured with 10 Hz frequency during the tests. If vertical load is not used the lateral load is applied continuously and the load and displacements are measured.

Each specimen is loaded, unloaded then loaded in the other direction and unloaded again, to get one cycle of the F_i–U_i relationship, including the deformation of the specimen's components and the sliding of the sliding clip. The used subscript in this paragraph $i = T, B$.

3 Experimental results

3.1 Typical behaviour modes

The typical behaviours of the specimens are presented in this section to illustrate the characteristics of the different standing seam roof parameters. Typical F–U relationships are shown in Fig. 7, when the upper flange is laterally loaded and no vertical load is applied on the specimen. Fig. 7/a shows the typical results without bridge system and Fig. 7/b represents the specimen with bridge system. In this case the main part of the displacement is gained from the deformation of the purlin and the bridge if applied. There are no sliding effects recognized in case of this structural layout, which can be related to the stack of the moving part of the sliding clips due to its deformation. The stiffness of the specimens using bridge systems is much smaller (10-20%)
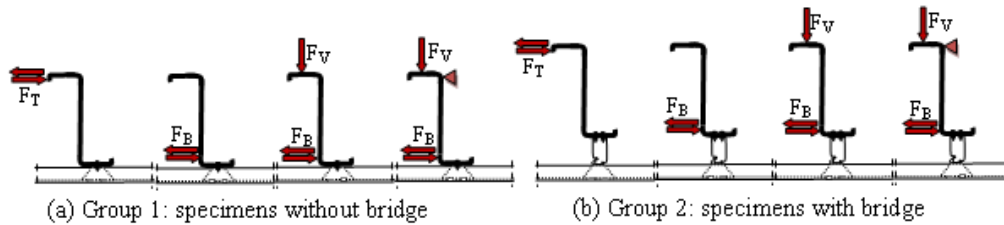
(a) Group 1: specimens without bridge   (b) Group 2: specimens with bridge

Fig. 4. Test arrangements and loading conditions.
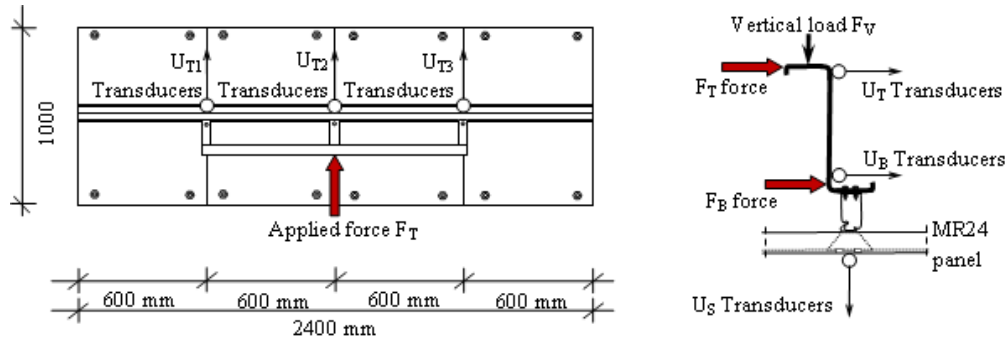
Fig. 5. Loading conditions and the measuring system.

Fig. 6. Test arrangement.

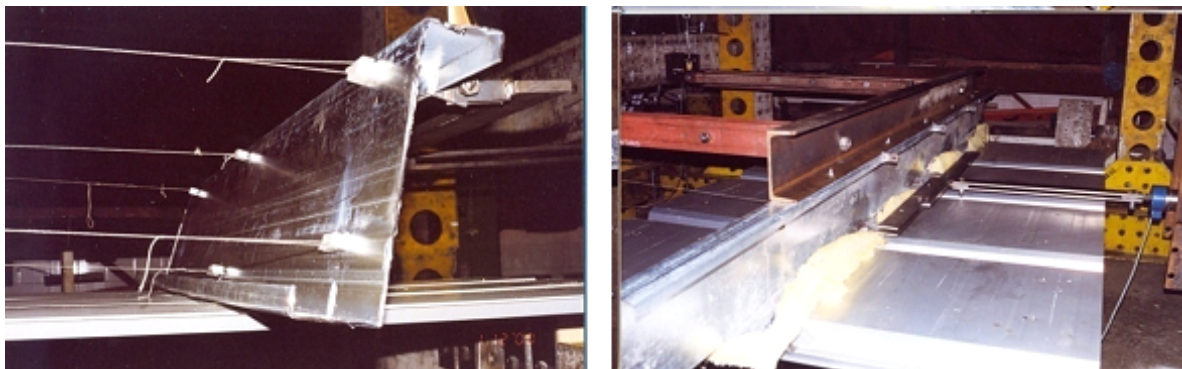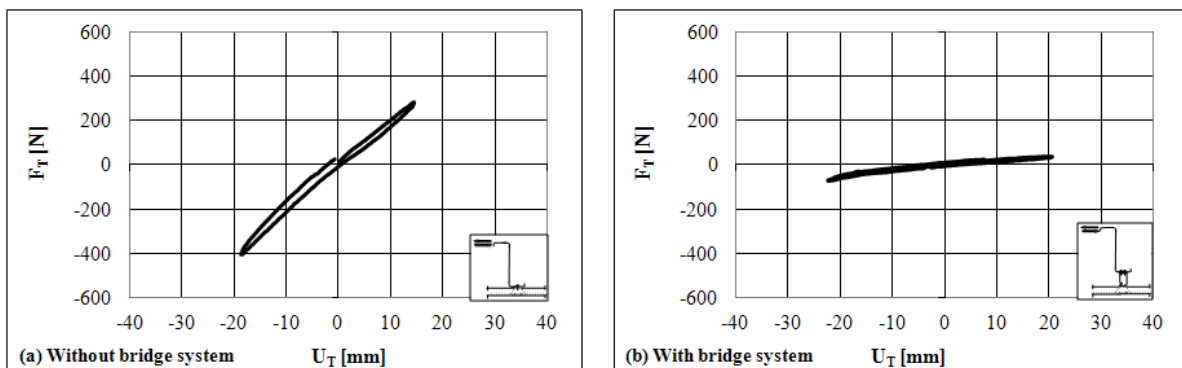(a) Without bridge system U_T [mm]   (b) With bridge system U_T [mm]

Fig. 7. F_T–U_T relationship for loading type 1.

or (0,00143 N/mm^2) comparing to specimens with only sliding clips (0,0083 N/mm^2), due to the deformation of the bridge clip.

In Fig. 8 the typical F–U relationship is shown if the lower flange is loaded laterally without vertical loads. In this case smooth sliding occurs after slight deformation of the purlin, if specimens are built without bridge systems. The overloading of specimens results hardening in both loading directions due to the contact in the connection between the sliding clip and the panel at folding of the seaming of the components (Fig. 8/a).

If specimens are built with bridge system, the same behaviour occurred as in the case of loading type 1 (Fig. 8/b). The deformation of the Z-purlin and the bridge system causes the sliding clip to stack and it is preventing the sliding action.

When vertical load is applied the sliding effect becomes dominant, as shown in Fig. 9. Gravity load stabilizes the specimen and decreases the deformation of the components, and the sliding part of clip is able to move under the lateral load effect. In the same time the gravity load increases the friction force what
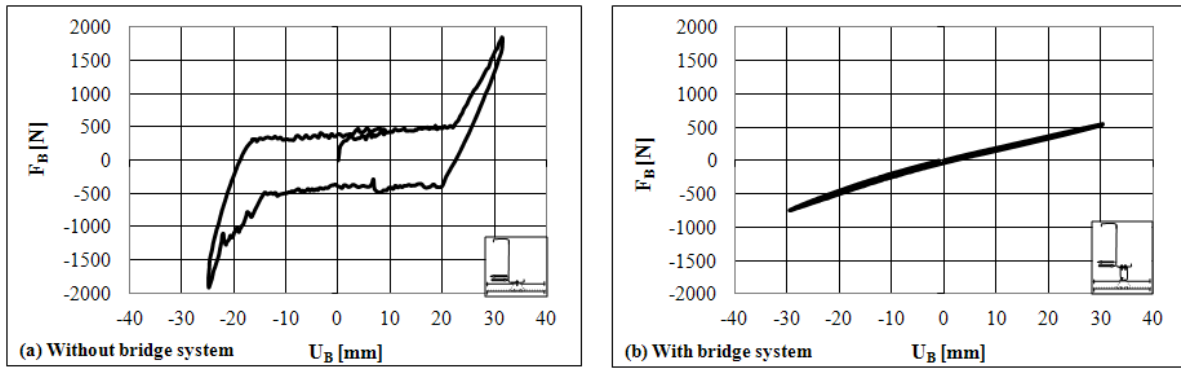
Fig. 8. F_B-U_B relationship for loading type 2.

can explain the stick and slip nature of the sliding action, when the friction/sliding force is reached sliding take place in the form of a jump.

If the upper flange is restrained the behaviour is similar to the previous case with sliding, having higher saw teeth related to the higher friction force due to the vertical load and the restrain effect of the upper flange, as it is shown in Fig. 10.

3.2 Deformation components

The recorded displacements reached due to the applied loads are composed of the following deformation components:

D_{sh} – MR24 sheeting deformation,

D_{cl} – clip deformation,

D_{pu} – purlin deformation,

D_{br} – bridge deformation.

Based on the test observations the deformation of the sheeting (D_{sh}) and the clip (D_{cl}) are not significant. Main part of the deformation comes from the bridge (D_{br}) and purlin (D_{pu}) deformations, as shown in Fig. 11.

In the previous behaviour modes three classes of slip types can be classified:

1. F_T-U_T relationship, without slip (Fig. 7),

2. F_B-U_B relationship, with smooth slip (S_{sm} slip type in Fig. 12/b),

3. F_B-U_B relationship with continuous stick–slip after the first slip happened (S_{sc} slip type in Fig. 12/c).

In case of behaviour with sliding action the slip starts at a certain load level (S_{in} – initial slip), what is called initial sliding force, as shown in Fig. 12/a.

4 Lateral Stiffness of Purlin-Panel Interaction

4.1 Lateral stiffness model without sliding action

The lateral stiffnesses are obtained from the results of standardized experimental results following Eq. 1, as it is recommended by EN 1993-1-3 [6] if the lower flange of the purlin is loaded laterally. The model characteristics in this case are taking the free flange of the purlin (lower flange) with a web part h/6 into account, where h is the height of the Z-purlin, as shown in Fig. 13. The model considers this part of the purlin as a beam continuously supported by springs. The spring coefficient includes the characteristics of the neglected part of the purlin with dashed line.

The spring coefficient K can be obtained by the proposed method of EN 1993-1-3 [6], according to Eq. 1. The necessary parameters for this model are taken from experimental results.

$$K = \frac{1}{\frac{1}{K_A} + \frac{1}{K_B}} = \frac{F}{U} \tag{1}$$

Where:

F load per unit length to produce a lateral displacement h/10,

U lateral displacement of the top flange in the loading direction,

K_A lateral stiffness per unit length corresponding to the rotational stiffness of the connection between the sheeting and the purlin,

K_B lateral stiffness per unit length due to distortion of the purlin cross-section,

K lateral stiffness per unit length achieved from loading the free lower flange of the purlin laterally as shown in Fig. 13 (in the presented study the free flange is the upper one as it is shown in the experimental layout in Fig. 5).

Herein the lateral stiffness is calculated for all the analysed specimens loaded at the upper flange. The average values of the results are summarised in Tab. 1, classified according to the purlin height, bridge system and load direction. The positive load direction is taken when the load is applied in the direction toward the purlin web and the negative load in the opposite direction. The stiffness values are calculated and evaluated separately according to the loading direction as well.

As experienced during the tests the lateral stiffness cannot be determined in this direct way for specimens with sliding, this is why it is necessary to define other parameters to be able to determine the deformation characteristics of the roof system.

4.2 Lateral stiffness model with sliding action

Sliding action is experienced after the linear deformation of the purlin (D_{pu}) and the bridge (D_{br}) in both positive and negative loading directions when specimens are loaded at the lower flange level. Due to the sliding the lateral stiffness interpretation is different comparing to the previous case. Because of the
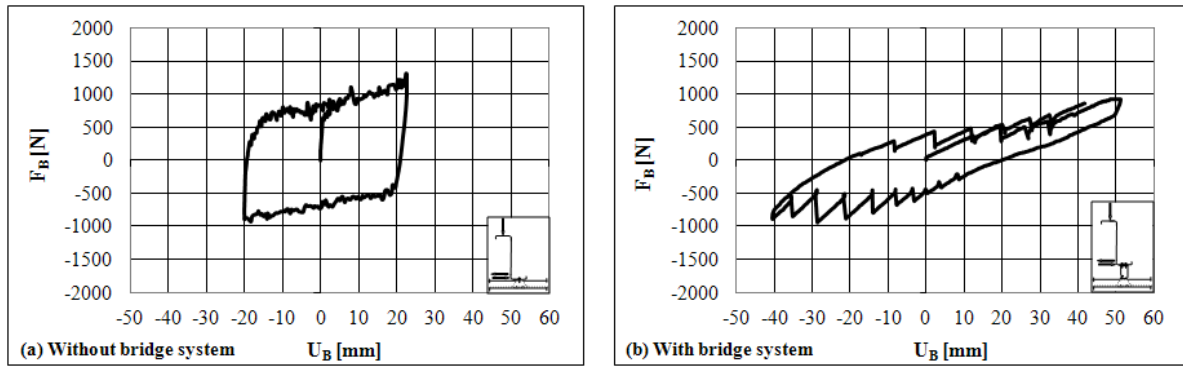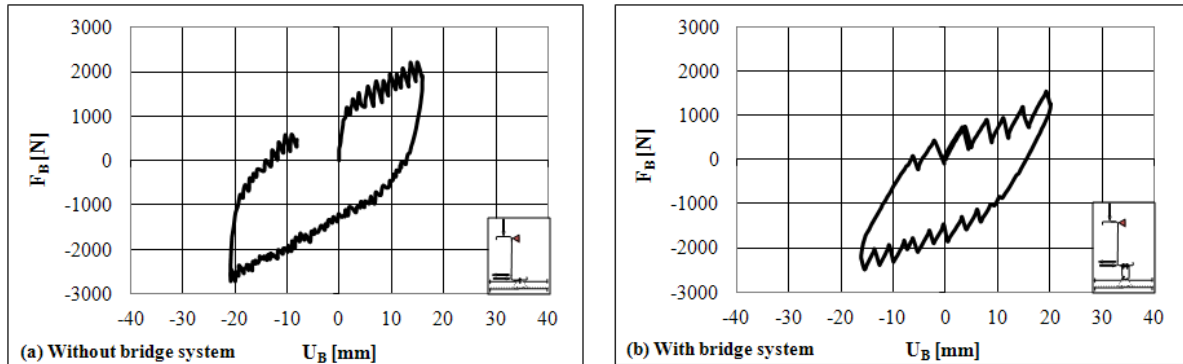
Fig. 9. F_B–U_B relationship for loading type 3.

Fig. 10. F_B–U_B relationship for loading type 4.

Tab. 1. Average stiffnesses of the specimens.

	bridge	purlin	$K \times 100$ [N/mm^2] loaded in positive direction	$K \times 100$ [N/mm^2] loaded in negative direction
	–	Z-200	0.83	0.85
	–	Z-250	0.74	0.954
	used	Z-200	0.143	0.143
	used	Z-250	0.061	0.124

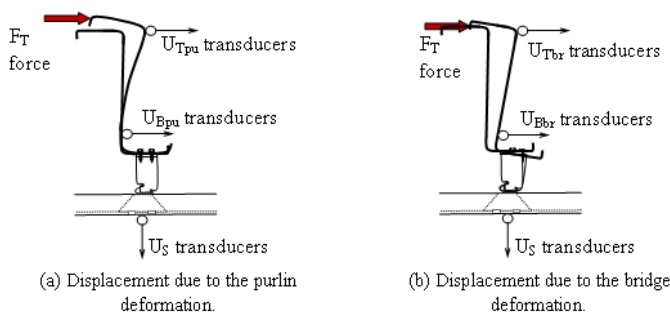different characteristics of the structural behaviour an enhanced model is developed.

Fig. 11. Main deformation components.

On the basis of the typical F_B–U_B relationship and having the above detailed conditions, the characteristics of the structural behaviour are determined in the form of physical parameters based on the experimental results. These parameters characterise the lateral stiffness model, as shown in Fig. 14.

The parameters of the lateral stiffness model are characterised by the elastic lateral stiffness K_1, the sliding stiffness K_2 and the initial sliding force F_f. The definitions of these parameters are as follows:

K_1 Average elastic lateral stiffness of the system (it is taken for three parts of F_B–U_B relationship), which can be calculated from Eq. 2.

K_2 Friction/sliding stiffness of the system including nonlinear behaviour and sliding effects, which can be calculated from Eq. 3.

F_f Average initial friction/sliding load at which sliding and nonlinear behaviour occurs, which can be calculated from Eq. 4.

In the derivation of the model parameters there are several uncertainties especially due to the sliding phenomenon. Therefore during the evaluation of the test results, to predict the values of the model parameters it is necessary to take the measured values at more positions on the F_B–U_B diagrams to calculate the average values and to determine the model parameters according to Eqs. 2-7.

$$K_1 = \frac{K_{11} + K_{12} + K_{13}}{3} \qquad (2)$$

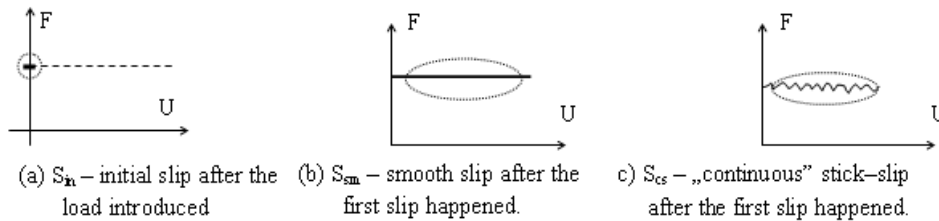$$K_2 = \frac{\frac{F_{max} - F_{min}}{L}}{U_{max} - U_{min}} \qquad (3)$$

(a) S_{in} – initial slip after the load introduced

(b) S_{sm} – smooth slip after the first slip happened.

c) S_{cs} – „continuous" stick–slip after the first slip happened.

Fig. 12. Interpretation of the slip types.

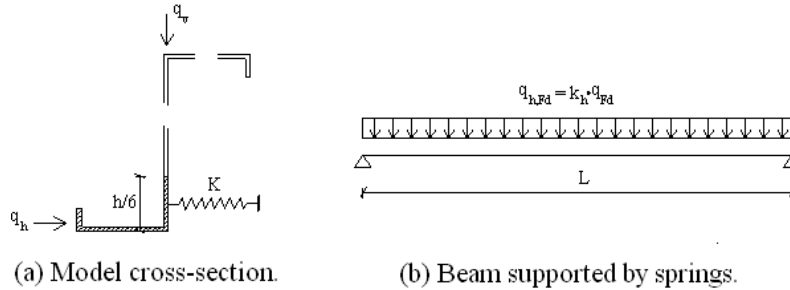(a) Model cross-section.

(b) Beam supported by springs.

Fig. 13. Laterally supported beam model of EN 1993-1-3 [6].

$$F_f = \frac{|F_{T1} - F_{T2}| + |F_{T3} - F_{T4}|}{4} \qquad (4)$$

The initial stiffness:

$$K_{11} = \frac{\frac{F_{min}}{L}}{U_{min}} \qquad (5)$$

The unloading stiffness:

$$K_{12} = \frac{\frac{F_3 - F_4}{L}}{U_3 - U_4} \qquad (6)$$

The reloading stiffness:

$$K_{13} = \frac{\frac{F_1 - F_2}{L}}{U_1 - U_2} \qquad (7)$$

Where:

F_{min} force where the sliding of clips occurred, and U_{min} is the corresponding displacement,

F_{max} force at the end of clip sliding, and U_{max} is the corresponding displacement,

F_1, F_2 forces on the reloading path corresponding to the selected U_1 and U_2 displacements,

F_3, F_4 forces on the unloading path corresponding to the selected U_3 and U_4 displacements,

F_{T1}, F_{T2} forces corresponding to the selected U_{T1} and U_{T2} displacements,

F_{T3}, F_{T4} forces corresponding to the selected U_{T3} and U_{T4} displacements,

L span of the specimens.

4.3 Experimental lateral stiffnesses

The elastic lateral stiffness K_1, the sliding stiffness K_2 and the initial sliding force F_f are calculated according to the Eqs. 2-4, for all the analysed specimens. The average values are calculated for all test series with the same parameters and load conditions. The obtained values are summarized and presented in Tables 2-4, according to the loading type, magnitude of the vertical load, support conditions and usage of the bridge system.

Note that some values are missing from these tables; in Tab. 2 in case of specimens with bridge systems with upper flange unrestrained the specimen became unstable when 577 N/clip is applied; in Tab. 3 in one case sliding did not take place because of the deformation of the sliding part of the clip stacked; in Tab. 4 the nature of the F-U relationship (see Fig. 9/b) did not allow to determine the initial sliding force in all cases when one flange of purlin was free and having bridge system used.

The evaluation of these results and the determined tendencies are presented in the following section.

Tab. 2. Average elastic lateral stiffness of specimens.

upper flange condition	F_V [N/clip]	$K_1 \times 100$ [N/mm^2]			
		Z-200	Z-200	Z-250	Z-250
	0	0.164	0.009	0.1	0.005
	165	0.247	0.003	0.067	0.011
	427	0.275	0.004	0.176	0.022
	577	0.329	–	0.162	–
	165	0.269	0.08	0.226	0.064
	427	0.263	0.09	0.187	0.07
	577	0.306	0.085	0.196	0.077
	727	0.311	0.085	0.38	0.079

5 Evaluation of lateral stiffnesses

5.1 Purlin upper flange laterally loaded - stiffness without sliding

When the upper flange is loaded laterally and no vertical load is applied on the specimens (loading type 1), no sliding is observed during the tests. The lateral stiffness of the upper flange are determined for each specimen and presented in Tab. 1. These stiffnesses are compared to each other to emphasize the effect of
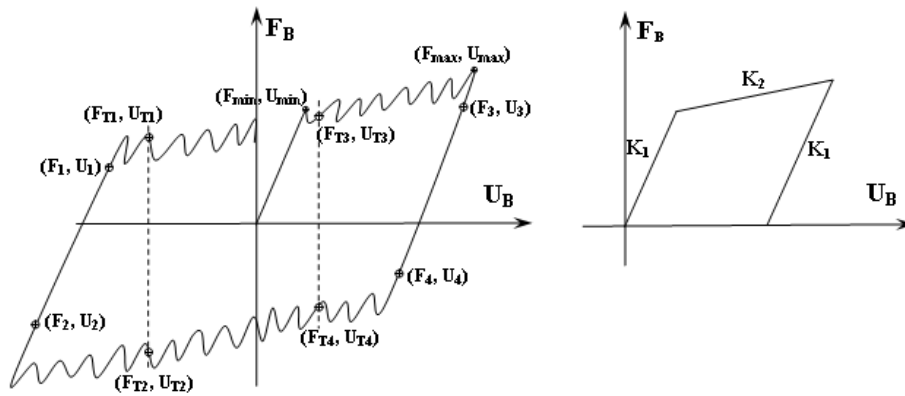
Fig. 14. Typical F_B–U_B relationship and the parameters of lateral stiffness model.

Tab. 3. Average sliding stiffness of the specimens.

upper flange condition	F_V [N/clip]	$K_2 \times 100$ [N/mm²]			
		Z-200	Z-200	Z-250	Z-250
⌐	0	0.003	0.0014	0.0025	–
	165	0.01	0.0003	0.0028	0.0058
	427	0.014	0.0013	0.0115	0.0128
	577	0.018	–	0.0094	–
⊲	165	0.054	0.0219	0.0353	0.0103
	427	0.044	0.0169	0.0346	0.003
	577	0.051	0.0145	0.0406	0.0135
	727	0.058	0.0147	0.034	0.0073

Tab. 4. Average initial sliding force of the specimens.

upper flange condition	F_V [N/clip]	$2F_f$ [N]			
		Z-200	Z-200	Z-250	Z-250
⌐	0	1072	–	859	–
	165	1430	169	458	–
	427	1812	–	1573	–
	577	1978	–	1900	–
⊲	165	2140	1314	1298	1580
	427	2083	2121	1693	2128
	577	2141	2524	1888	2459
	727	2713	3011	2080	3044

the purlin height, bridge system and the loading direction.

The lateral stiffness of specimen with Z-250 purlins is about 40–90% the stiffness of specimens with Z-200 purlins depending on the other structural elements used, as shown in Fig. 15/a. The lateral stiffness of the specimens with bridge system is about 10–20% the stiffness without bridge system (Fig. 15/b).

It is noted that there is a big scatter in the stiffness if different load directions are used: the lateral stiffness of the specimens loaded in positive direction is about 25–100% of the stiffness of specimens loaded in negative direction depending on the other applied structural elements.

5.2 Purlin lower flange laterally loaded - stiffness with sliding

The lateral stiffness of the lower flange is evaluated through the comparisons of all parameters of the proposed lateral stiffness model (K_1, K_2, and F_f). The values of these parameters are determined and presented in Tables 2-4. The comparisons are shown by diagrams to demonstrate the effect of the different parameters on the lateral stiffness. These effects are classified and presented by the components of specimens.

5.2.1 Initial elastic lateral stiffness K_1
- Purlin height effect

The initial elastic lateral stiffness with or without bridge system having both restrained and unrestrained cases of upper flange with Z-250 purlins are smaller than the stiffness of specimen with Z-200 purlins, as shown in Fig. 16.
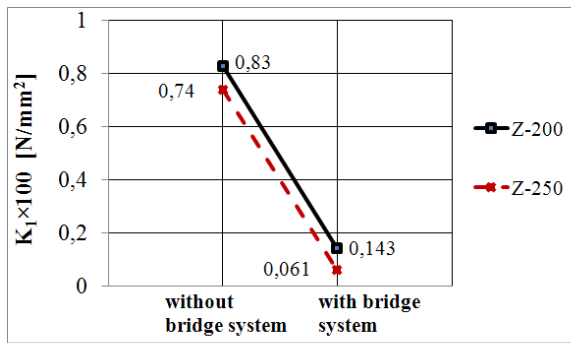
- Bridge system effect

The initial elastic lateral stiffness for Z-200 and for Z-250 purlins with bridge system is smaller than it is for specimens without bridge system. If the upper flange is unrestrained the effect is much higher. It is observed that the effect of the bridge is the most significant among all of the other parameters (stiffness of specimens with bridge system is about 1–40% of specimens without), as it is shown in Fig. 17. The experienced scatter can be explained by the sliding phenomenon.
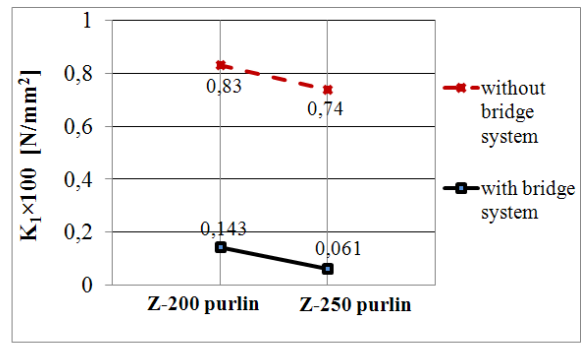
- Restrain effect

In case of unrestrained upper flange the stiffnesses are smaller than it is for purlins with restrained upper flange. The stiffnesses are higher if the gravity loads are increased, and in case of Z-250 with bridge system the effect is the most dominant, as shown in Fig. 18.

- Gravity load effect

The vertical load has stabilizing effect on the tested system, therefore the higher the gravity load the higher is the initial elastic lateral stiffness, as it can be seen in Fig. 19.

(a) Purlin height effect.   (b) Bridge effect.
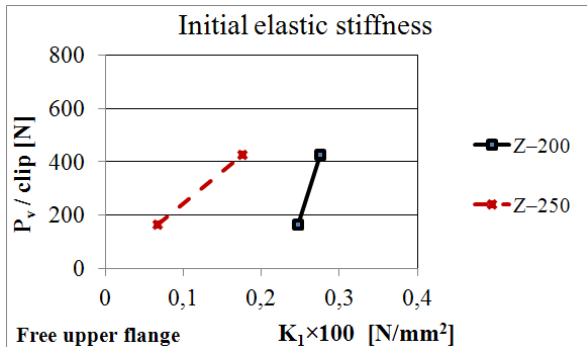
Fig. 15. Lateral stiffness of the upper flange.
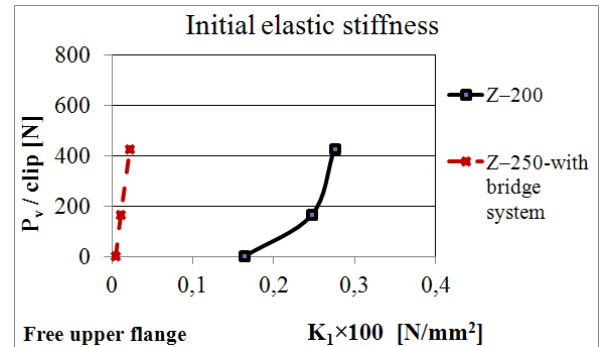

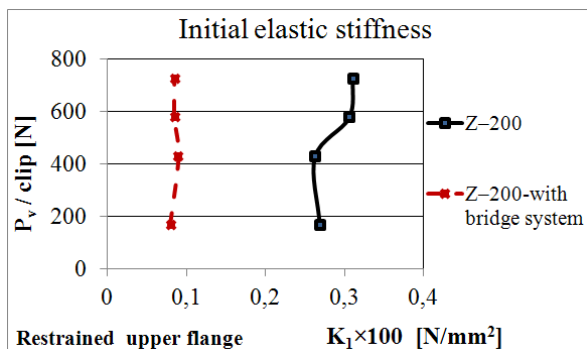**Fig. 16.** Purlin height effect.

Fig. 19. Gravity load effect.

Fig. 17. Bridge system effect.
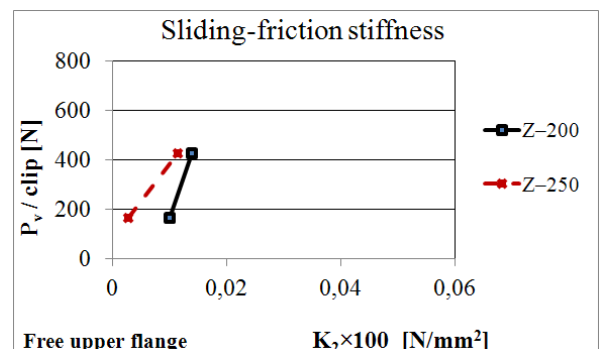

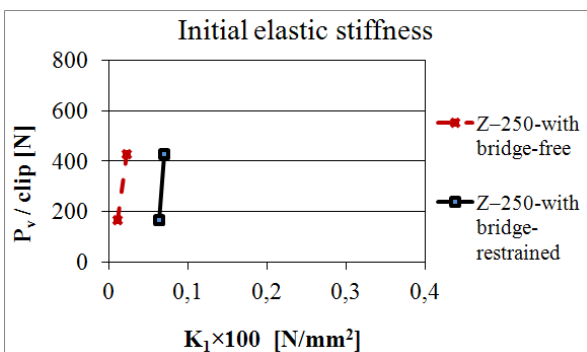**Fig. 20.** Purlin height effect.
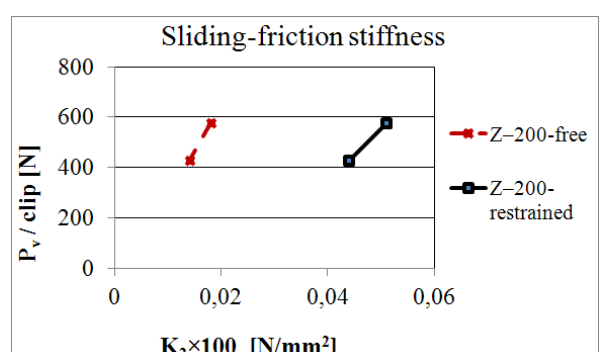

Fig. 18. Restrain effect.

Fig. 21. Restrain effect.

5.2.2 Sliding stiffness K_2

● Purlin height effect

The friction/sliding stiffnesses with or without bridge system having both restrained and unrestrained cases with Z-250 purlins are smaller than the stiffnesses of specimens with Z-200 purlins, as shown in Fig. 20.

● Bridge system effect

Similarly to the initial stiffness, the friction/sliding stiffness for Z-200 and for Z-250 purlins with bridge system is smaller than it is for specimens without bridge system, and if the upper flange is unrestrained this effect is much higher. For this stiffness the
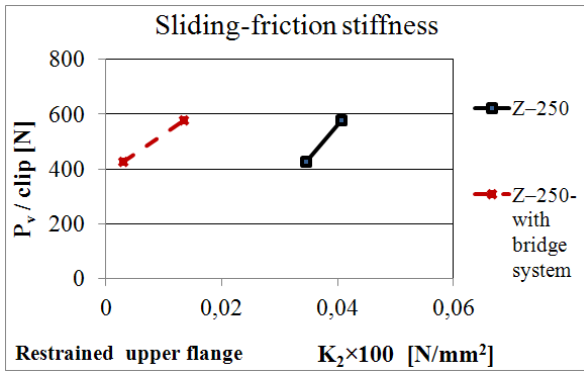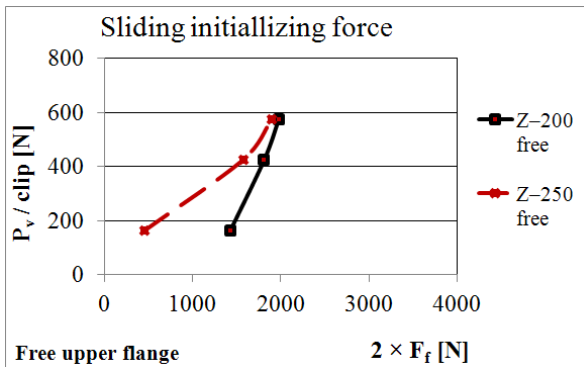
Fig. 22. Bridge system and gravity load effects.
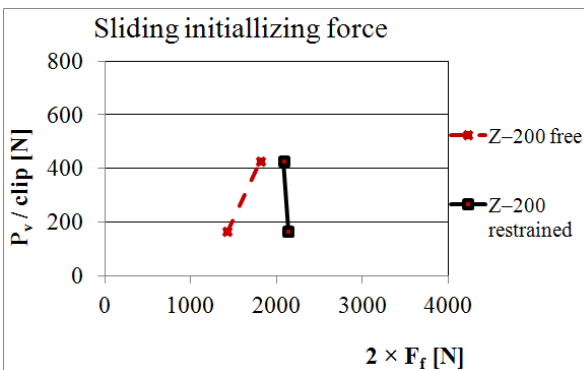

Fig. 23. Purlin height effect.

Fig. 24. Restrain effect.

effect of the bridge is also the most dominant: stiffness of specimens with bridge systems is about 5–50% of specimens without, as it is shown in Fig. 22.

- Restrain effect

In case of specimens with restrained/unrestrained upper flange the friction/sliding stiffness have the same tendencies as observed for the initial stiffness, as shown in Fig. 21.

- Gravity load effect

The gravity load has stabilizing effect and increases the friction, so the higher the gravity load the higher is the friction/sliding lateral stiffness, as shown in Fig. 22.

5.2.3 Initial sliding force F_f
- Purlin height effect

The initial sliding force with or without bridge system having both restrained and unrestrained cases of upper flange with Z-250 purlins are smaller than for specimens with Z-200 purlins. The ratio varies between 30–95%, as shown in Fig. 23.

- Bridge system effect

The initial sliding force for both purlins with bridge system is higher than for specimens without bridge system in case of restrained upper flange. If the upper flange of purlin is free the initial sliding force for both purlins with bridge system is smaller. This can be related to the deformation of bridge elements which is restrained by the support of the upper flange resulting higher initial sliding forces, as it is shown in Fig. 25/b. When the upper flange is free this restrain is not acting and bridge system has a decreasing effect on the initial sliding force, as shown in Fig. 25/a.

- Restrain effect

In case of unrestrained upper flange the initial sliding forces are smaller than for specimens with restrained upper flange. The initial sliding forces are higher with higher gravity loads and when the upper flange is restrained, as shown in Fig. 24. In case of Z-250 with bridge system the effect is much more significant.

- Gravity load effect

The gravity load effect is shown in Fig. 25; as it is expected the increased gravity load results in higher initial sliding force; the increasing amount is significant.

6 Summary and conclusions
6.1 Summary

An experimental study is completed to study the behaviour and the effect of sliding clips and bridge system on the lateral stiffness of standing seam roofs. The specimens are tested under various load and structural arrangements.

The test experiences and results show that the behaviour of the investigated structural detail is quite complex and contain several uncertainties due to especially to the sliding/friction in the sliding clip and to the deformation of the bridge system.

The calculated lateral stiffness values demonstrate clearly the tendencies and the effects of different structural details. The numerical values, however, have a big scatter what should be considered when these are used in the global analysis of purlins as supporting spring constants.

Using the proposed model the behaviour of specimens is evaluated. On this basis the effect of the different structural components and loads are determined.

6.2 Conclusions

In standard purlin–sheeting roofs (with direct screwed connection between purlin and trapezoidal sheeting) the purlin height has the biggest influence on the lateral stiffness, as it is shown in [7]. In the standing seam roof the major affect is by
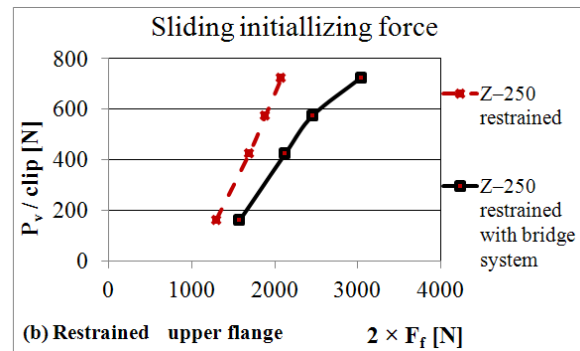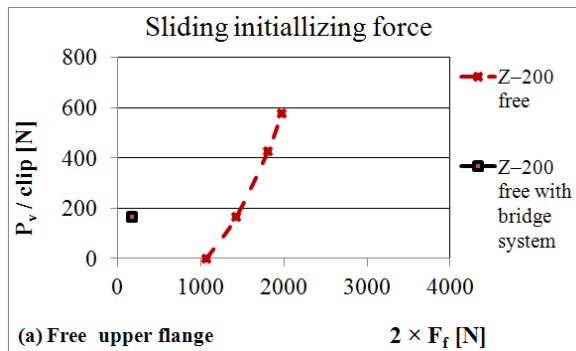
Fig. 25. Bridge system and gravity load effects.

the bridge systems. The bridge arrangement (especially its connection to the purlin) results in a weak lateral support between the adjacent components.

The sliding phenomenon of the sliding clip is a further uncertainty in the system. In the study a model is proposed how to interpret and determine the main characteristics of it, by the initial and sliding stiffness (K_1, K_2) and the initial sliding force (F_f).

By the evaluation of the results a big scatter of the model parameters is found due to the uncertainties in the phenomena. It is observed that, the effect of the bridge system has the largest influence on the structural behaviour. The stiffness for specimens with bridge system is about 10-40% comparing to specimens without bridge system. The effect of the purlin height is significant as well.

The test results called the attention on some insufficient structural details, which are redesigned by the industrial partner to improve the behaviour.

The effect of the experimentally derived parameters on the global behaviour are studied by the global analysis of purlins applied in the Z-purlin/MR24 cladding system, and on the basis of the results design method is developed [8]. The method is based on a 7 DOF's beam finite element, considering the warping effect. The cross-section distortion and the cladding deformation are considered in the model by elastic supports (lateral and rotational springs); the spring characteristics are determined on the basis of the experimental values. In the elastically supported beam model equivalent geometric imperfections are used and the design values of the stresses are calculated by geometrically nonlinear, imperfect analysis (GNIA).

References

1 **Serrette R, Peköz T**, *Bending strength of standing seam roof panels*, Thin-Walled Structures **27** (1997), no. 1, 55–64, DOI 10.1016/0263-8231(96)00018-3.

2 **Surry D, Sinno R R, Nail B**, *Structurally effective static wind loads for roof panels*, Journal of Structural Engineering ASCE **133** (June 2007), no. 6, 871–885, DOI 10.1061/(ASCE)0733-9445(2007)133:6(871).

3 **Farquhar S, Kopp G A, Surry D**, *Wind tunnel and uniform pressure tests of a standing seam metal roof model*, Journal of Structural Engineering ASCE **131** (April 2005), no. 4, 650–659, DOI 10.1061/(ASCE)0733-9445(2005)131:4(650).

4 **Hosam M, Senseny P**, *Models for standing seam roofs*, Journal of Wind Engineering and Industrial Aerodynamics **91** (December 2003), no. 12-15, 1689–1702, DOI 10.1016/j.jweia.2003.09.014.

5 **El Damatty A A, Rahman M, Ragheb O**, *Component testing and finite element modelling of standing seam roofs*, Thin walled structures **41** (November 2003), no. 11, 1053–1072, DOI 10.1016/S0263-8231(03)00048-X.

6 *EN 1993-1-3: Eurocode 3, Design of Steel Structures – Part 1-3: General rules Supplementary rules for cold-formed members and sheeting*, 2005.

7 **Kachichian M, Dunai L, Kaltenbach L, Kálló M**, *Experimental study on the interaction of steel sheeting and Z-purlins*, 6th International Colloquium on Stability and Ductility of Steel Structures (Timisoara, Romania, September 09, 1999), Stability and Ductility of Steel Structures (SDSS'99) (Dubina D, Iványi M, eds.), Elsevier, 1999, pp. 293–306.

8 **Werner F**, *Design method for thin-walled, cold-formed load bearing elements – CFDM for the ASTRON light steel building system*, Institute of Construction, Bauhaus University, Weimar, July 2008.